SEARCH FOR THE QCD CRITICAL POINT BY HIGHER MOMENTS OF NET-PROTON MULTIPLICITY DISTRIBUTIONS AT RHIC*

Xiaofeng Luo

for the STAR Collaboration

Institute of Particle Physics, Central China Normal University
Wuhan 430079, China
and
Key Laboratory of Quark and Lepton Physics, Central China Normal University
Ministry of Education, Wuhan 430079, China

(Received November 28, 2011)

Higher moments of net-proton multiplicity distributions are applied to search for the QCD critical point. In this paper, we will present measurements for kurtosis (κ), skewness (S) and variance (σ^2) of net-proton multiplicity distributions at the mid-rapidity ($|y| < 0.5$) and transverse momentum range $0.4 < p_{\rm T} < 0.8$ GeV/c for Au+Au collisions at $\sqrt{s_{_{NN}}} =$ 7.7, 11.5, 39, 62.4 and 200 GeV, Cu+Cu collisions at $\sqrt{s_{_{NN}}} =$ 22.4, 62.4 and 200 GeV, and p+p collisions at $\sqrt{s_{_{NN}}} =$ 62.4 and 200 GeV. The moment products $\kappa\sigma^2$ and $S\sigma$ of net-proton distributions, which are related to volume independent baryon number susceptibility ratios, are consistent with Lattice QCD and Hadron Resonance Gas (HRG) model calculations at high energies ($\sqrt{s_{_{NN}}} =$ 62.4 and 200 GeV). Deviations of $\kappa\sigma^2$ and $S\sigma$ for the Au+Au collisions at low energies ($\sqrt{s_{_{NN}}} =$ 7.7, 11.5 and 39 GeV) from HRG model calculations are also observed.

DOI:10.5506/APhysPolBSupp.5.497
PACS numbers: 25.75.Ld, 25.75.Dw

1. Introduction

The main goal of Beam Energy Scan (BES) program [1] at the Relativistic Heavy Ion Collider (RHIC) is to study the phase structure [2], such as map the QCD phase boundary and search for the QCD critical point [3], of

* Presented at the Conference "Strangeness in Quark Matter 2011", Kraków, Poland, September 18–24, 2011.

the QCD matter created in heavy ion collision. By tuning the colliding energies of two nuclei from $\sqrt{s_{NN}}$= 200 GeV to $\sqrt{s_{NN}}$= 7.7 GeV, we can access various region of the QCD phase diagram. Higher moments (variance (σ^2), skewness (S), kurtosis (κ) *etc.*) of conserved quantities, such as net-baryon, net-charge and net-strangeness, multiplicity distributions are very sensitive to the correlation length [4, 5] and can be directly connected to the corresponding thermodynamic susceptibilities in Lattice QCD [6, 7] and Hadron Resonance Gas (HRG) model [8]. As the volume of the system is hard to determine, the susceptibility ratio, such as $\chi_B^{(4)}/\chi_B^{(2)}$ and $\chi_B^{(3)}/\chi_B^{(2)}$, are used to compare with the experimental data as $\kappa\sigma^2 = \chi_B^{(4)}/\chi_B^{(2)}$ and $S\sigma = \chi_B^{(3)}/\chi_B^{(2)}$. Theoretical calculations demonstrate that the experimental measurable net-proton (proton number minus anti-proton number) number fluctuations can effectively reflect the fluctuations of the net-baryon number [9]. Higher moments analysis opens a completely new domain and provides quantitative method for probing the bulk properties of the hot dense nuclear matter [2].

2. Observables

Experimentally, we measure net-proton number event-by-event wise, $N_{p-\bar{p}} = N_p - N_{\bar{p}}$, which is proton number minus antiproton number. In the following, we use N to represent the net-proton number $N_{p-\bar{p}}$ in one event. The average value over whole event ensemble is denoted by $\mu = \langle N \rangle$, where the single angle brackets are used to indicate ensemble average of an event-by-event distributions. The deviation of N from its mean value are defined by

$$\delta N = N - \langle N \rangle = N - \mu \,. \tag{1}$$

The r-th order central moments are defined as

$$\mu_r = \langle (\delta N)^r \rangle \,, \qquad \mu_1 = 0 \,. \tag{2}$$

Then, we can define various order cumulants of event-by-event distributions as

$$C_1 = \mu \,, \qquad C_2 = \mu_2 \,, \qquad C_3 = \mu_3 \,, \tag{3}$$

$$C_n (n > 3) = \mu_n - \sum_{m=2}^{n-2} \left(\begin{array}{c} n-1 \\ m-1 \end{array} \right) C_m \mu_{n-m} \,. \tag{4}$$

Once we have the definition of cumulants, various moments can be denoted as

$$M = C_1 \,, \qquad \sigma^2 = C_2 \,, \qquad S = \frac{C_3}{(C_2)^{3/2}} \,, \qquad \kappa = \frac{C_4}{(C_2)^2} \,. \tag{5}$$

Then, the moments product $\kappa\sigma^2$ and $S\sigma$ can be expressed in term of cumulant ratio

$$\kappa\sigma^2 = \frac{C_4}{C_2}\,, \qquad S\sigma = \frac{C_3}{C_2}\,. \tag{6}$$

3. Background effects

Therminator model [10] was applied to study the resonance decay effect, which is a background effect for higher moment analysis, and also to check whether the net-proton fluctuations can reflect the net-baryon number fluctuations. In Fig. 1 (left), we show the event-by-event number distributions of Au+Au 0–5% most central collisions at $\sqrt{s_{NN}} = 200$ GeV from Therminator calculations for four cases. Fig. 1 (left) demonstrates that the distribution for the net-proton with resonance decay is wider than the net-proton distributions without decay. By excluding the Λ decay nucleon, the net-(proton+neutron+Λ) has narrower distribution than the net-(proton+neutron) distributions. Fig. 1 (right) shows centrality dependence of $\kappa\sigma^2$ of number distributions. The results for the four cases are consistent with each other within errors, which indicate the effects of resonance decay are small and the net-proton fluctuations can reflect the net-baryon fluctuations. The statistical errors are evaluated by Delta theorem method [11].

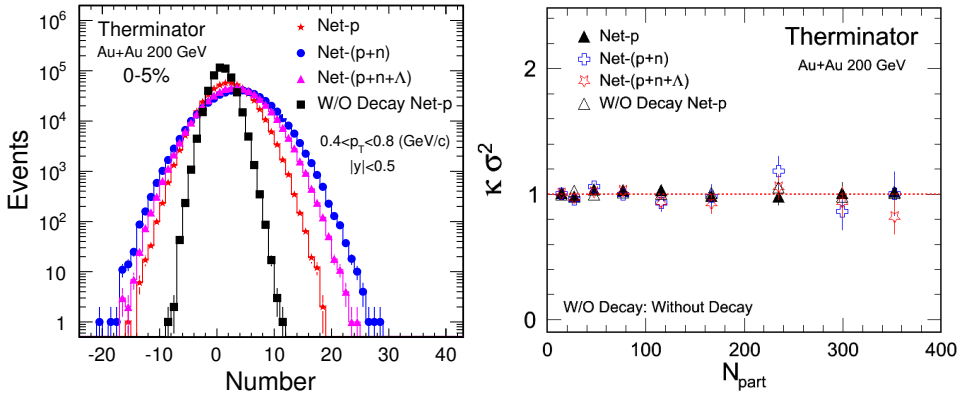

Fig. 1. Left: Event-by-event number distributions for net-proton, net-(proton+neutron), net-(proton+neutron+Λ) and net-proton without resonance decay for 0–5% most central Au+Au collisions at $\sqrt{s_{NN}} = 200$ GeV from Therminator model. Right: Centrality dependence of $\kappa\sigma^2$ of number distributions of four cases for Au+Au collisions at $\sqrt{s_{NN}}$=200 GeV from Therminator model.

4. Experimental method

The data presented in this paper are obtained using the Solenoidal Tracker at RHIC (STAR). The main subsystem used in this analysis is a large, uniform acceptance cylindrical Time Projection Chamber (TPC) covering a pseudo-rapidity range of $|\eta| < 1$ and full azimuthal coverage. To ensure the purity and similar efficiency, the protons and anti-protons are identified with the ionization energy loss (dE/dx) measured by the TPC of STAR detector within $0.4 < p_{\mathrm{T}} < 0.8\,\mathrm{GeV}/c$ and mid-rapidity ($|y| < 0.5$). Centralities are determined by the uncorrected charged particle multiplicities ($dN_{\mathrm{ch}}/d\eta$) within pseudo-rapidity $|\eta| < 0.5$ measured by the TPC and the centrality bin width correction is used to eliminate volume fluctuations [12]. By comparing measured $dN_{\mathrm{ch}}/d\eta$ with the Monte Carlo Glauber model results, we can obtain the average number of participant (N_{part}) for each centrality.

5. Results

In this section, we present beam energy and system size dependence of various moments (M, σ, S, κ) and moment products ($S\sigma$ and $\kappa\sigma^2$) of net-proton distributions. Those are Au+Au collisions at $\sqrt{s_{NN}}$ = 7.7, 11.5, 39, 62.4 (year 2004) and 200 GeV (year 2004), Cu+Cu collisions at $\sqrt{s_{NN}}$ = 22.4, 62.4, 200 GeV, and $p + p$ collisions at $\sqrt{s_{NN}}$ = 62.4 (year 2006), 200 GeV (year 2009). The results for Au+Au collisions at $\sqrt{s_{NN}}$ = 62.4 and 200 GeV have been published in the paper [13]. The errors shown in the figures are statistical error only. Centrality dependence of various moments of net-proton distributions for Au+Au, Cu+Cu and p+p collisions are shown in Fig. 2 (left) and Fig. 2 (right), respectively. The M and σ are found to be monotonically increasing with increasing of N_{part}, while the S and κ are decreasing. The various moments can be well described by the dashed lines shown in the figures, which are derived from Central Limit Theorem (CLT) by assuming the colliding system consists of many identical and independent emission sources [12,14]. Energy dependence of $S\sigma$ and $\kappa\sigma^2$ for 0–5% most central Au+Au collisions are shown in Fig. 3. We find that the data are consistent with Lattice QCD and HRG model calculations at high energies ($\sqrt{s_{NN}}$ = 62.4 and 200 GeV), while deviations from HRG model are observed at low energies ($\sqrt{s_{NN}}$ = 7.7, 11.5 and 39 GeV). The possible reasons for the deviations are discussed in [15,16].

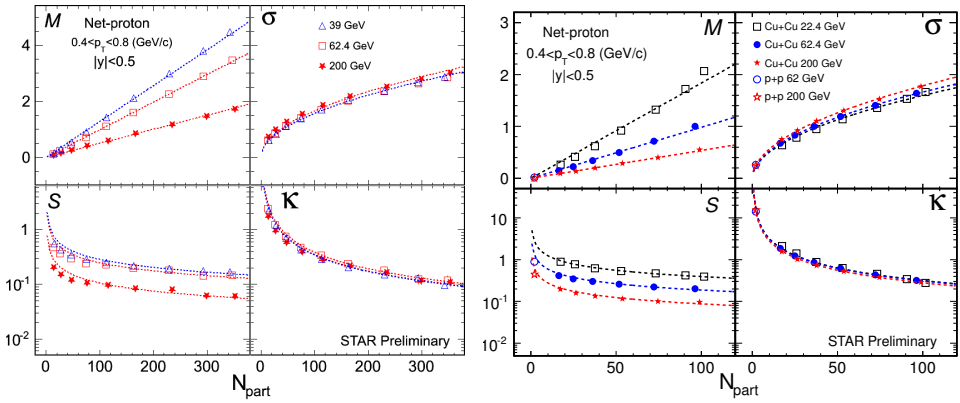

Fig. 2. Left: Centrality dependence of various moments of net-proton multiplicity distributions for Au+Au collisions at $\sqrt{s_{NN}}$ = 39, 62.4, 200 GeV. The dashed lines shown in the figure are expectation lines from CLT. Right: Centrality dependence of various moments of net-proton distributions for Cu+Cu collisions at $\sqrt{s_{NN}}$ = 22.4, 62.4 and 200 GeV and p+p collisions at $\sqrt{s_{NN}}$ = 62.4 and 200 GeV. The dashed lines shown in the figure are expectation lines from CLT.

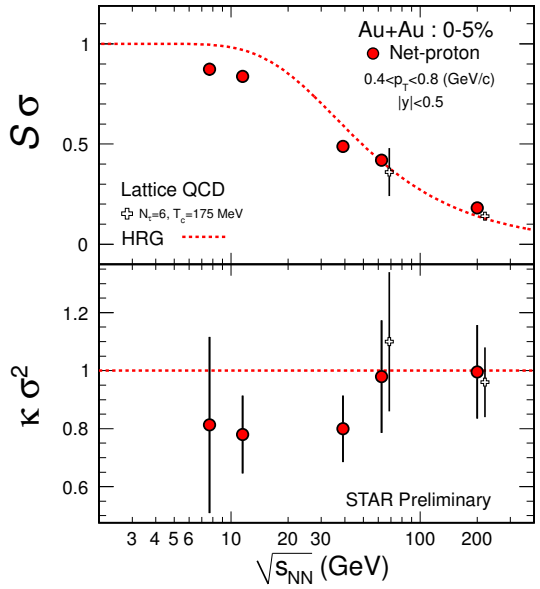

Fig. 3. Energy dependence of moment products ($\kappa\sigma^2$ and $S\sigma$) of net-proton distributions for 0–5% most central Au+Au collisions. The dashed lines (red) denote the HRG model calculations, and the empty markers denote Lattice QCD results [2].

6. Summary and outlook

Higher moments of net-proton distributions are applied to search for the QCD critical point and probe the bulk properties of QCD matters. In summary, we present the measurements of higher moments of net-proton distributions for Au+Au, Cu+Cu, and p+p collisions from STAR experiment. The moment products $\kappa\sigma^2$ and $S\sigma$ of net-proton distributions from 0–5% most central Au+Au collisions are consistent with Lattice QCD and HRG model calculations at high energies ($\sqrt{s_{NN}}$= 62.4 and 200 GeV), while the results are smaller than HRG model calculations at low energies ($\sqrt{s_{NN}}$= 7.7, 11.5, 39 GeV). The analysis of data from another two energies at $\sqrt{s_{NN}}$ = 19.6 and 27 GeV, which were collected in the year 2011, are ongoing.

The work was supported in part by the National Natural Science Foundation of China under grant No. 11135011.

REFERENCES

[1] M.M. Aggarwal *et al.* [STAR Collaboration], `arXiv:1007.2613v1 [nucl-ex]`.
[2] S. Gupta *et al.*, *Science* **332**, 1525 (2011).
[3] R.V. Gavai, S. Gupta, *Phys. Rev.* **D78**, 114503 (2008).
[4] M.A. Stephanov, *Phys. Rev. Lett.* **102**, 032301 (2009).
[5] C. Athanasiou *et al.*, *Phys. Rev.* **D82**, 074008 (2010).
[6] R.V. Gavai, S. Gupta, *Phys. Lett.* **B696**, 459 (2011).
[7] M. Cheng *et al.*, *Phys. Rev.* **D79**, 074505 (2009).
[8] F. Karsch, K. Redlich, *Phys. Lett.* **B695**, 136 (2011).
[9] Y. Hatta, M.A. Stephanov, *Phys. Rev. Lett.* **91**, 102003 (2003).
[10] A. Kisiel *et al.*, *Comput. Phys. Commun.* **174**, 669 (2006).
[11] X. Luo, *J. Phys. G: Nucl. Part. Phys.* **39**, 025008 (2012).
[12] X. Luo, *J. Phys.: Conf. Ser.* **316**, 012003 (2011).
[13] M.M. Aggarwal *et al.* [STAR Collaboration], *Phys. Rev. Lett.* **105**, 022302 (2010).
[14] X. Luo *et al.*, *J. Phys. G: Nucl. Part. Phys.* **37**, 094061 (2010).
[15] M.A. Stephanov, *Phys. Rev. Lett.* **107**, 052301 (2011).
[16] B. Friman *et al.*, *Eur. Phys. J.* **C71**, 1694 (2011).